



Explore the spatial pattern of carbon emissions in urban functional zones: a case study of Pudong, Shanghai, China

Enyan Zhu¹ · Jian Yao¹ · Xinghui Zhang² · Lisu Chen²

Received: 14 September 2023 / Accepted: 17 November 2023 / Published online: 5 December 2023
© The Author(s), under exclusive licence to Springer-Verlag GmbH Germany, part of Springer Nature 2023

Abstract

It is crucial for the development of carbon reduction strategies to accurately examine the spatial distribution of carbon emissions. Limited by data availability and lack of industry segmentation, previous studies attempting to model spatial carbon emissions still suffer from significant uncertainty. Taking Pudong New Area as an example, with the help of multi-source data, this paper proposed a research framework for the amount calculation and spatial distribution simulation of its CO₂ emissions at the scale of urban functional zones (UFZs). The methods used in this study were based on mapping relations among the locations of geographic entities and data of multiple sources, using the coefficient method recommended by the Intergovernmental Panel on Climate Change (IPCC) to calculate emissions. The results showed that the emission intensity of industrial zones and transport zones was much higher than that of other UFZs. In addition, Moran's *I* test indicated that there was a positive spatial autocorrelation in high emission zones, especially located in industrial zones. The spatial analysis of CO₂ emissions at the UFZ scale deepened the consideration of spatial heterogeneity, which could contribute to the management of low carbon city and the optimal implementation of energy allocation.

Keywords Urban carbon emissions · Multi-source data · Urban functional zone · Spatial analysis · Autocorrelation

Abbreviations

UFZ	Urban functional zone	NPP-VIIRS	National Polar-orbiting Operational Environmental Satellite System Preparatory Project Visible Infrared Imaging Radiometer Suite
IPCC	Intergovernmental Panel on Climate Change	POI	Point-of-interest
LMDI	Logarithmic mean Divisia index	OSM	OpenStreetMap
LEAP	Long-range Energy Alternatives Planning	ESDA	Exploratory spatial data analysis
DMSP-OLS	Defense Meteorological Satellite Program—Operational Linescan System	LISA	Local Indicators of Spatial Association
		ID	Industrial zone
		TS	Transport zone
		RS	Residential zone
		CT	Cultural tourism zone
		CS	Commercial service zone
		PS	Public service zone

Responsible Editor: V.V.S.S. Sarma

✉ Enyan Zhu
eyzhu@zju.edu.cn

Jian Yao
jyao0717@163.com

Xinghui Zhang
357602213@qq.com

Lisu Chen
lschen@shmtu.edu.cn

¹ College of Transport and Communications, Shanghai Maritime University, Shanghai 201306, China

² College of Ocean Science and Engineering, Shanghai Maritime University, Shanghai 201306, China

Introduction

Urban is the center of human activities that have a significant impact on the surface of the Earth. Rapid urbanization not only causes significant changes in the utilization of land but also concentrates intensive energy consumption, both of which release large amounts of CO₂ into the atmosphere. Some research showed that urban areas account for about 75% of carbon emissions worldwide (Li et al. 2022).

Moreover, the United Nations Habitat predicts that the proportion of urban carbon emissions will increase to 76% by 2030 (Gan et al. 2022). Therefore, the mitigation of urban carbon emissions has played a vital role in the process of global carbon reduction (Gong et al. 2022a).

Numerous studies have been conducted on urban carbon emissions at different scales, such as Peng used logarithmic mean Divisia index (LMDI) method to analyze the energy consumption of CO₂ emissions in Hunan province based on the Long-range Energy Alternatives Planning (LEAP) system model (Wang et al. 2017). Hu set up four scenarios to forecast and analyze the energy production and consumption of Shenzhen, a postindustrial city, from 2015 to 2030 (Hu et al. 2019).

However, similar studies regarded the city as a whole, but have no idea about the specific source and spatial distribution of carbon emissions. Some scholars used statistical data to compare the spatial heterogeneity between different administrations, and these studies generally concentrated on regions with low spatial resolution (Gan et al. 2022; Xia and Yang 2022). In recent years, the spatial study of urban carbon emissions has become an important research hotspot with the advancement of remote sensing technology and the abundance of multi-source data (AbdelRahman et al. 2021; Yang et al. 2022). The Defense Meteorological Satellite Program–Operational Linescan System (DMSP-OLS), a visible imaging linear scanning service system carried by the US Defense Meteorological Satellite, can obtain the weak light intensity on the ground (Wang et al. 2017; Zhang et al. 2022), which has been widely applied to carbon emission estimation. For example, Oda et al. used DMSP-OLS data to invert carbon footprint in city regions and used demographic data as an auxiliary inversion to non-city regions to generate a global carbon footprint grid map with 1-km spatial resolution from 2000 to 2019 (Oda and Maksyutov 2011). Based on National Polar-orbiting Operational Environmental Satellite System Preparatory Pro Visible Infrared Imaging Radiometer Suite (NPP-VIIRS) nighttime light remote sensing data, Narit found that the factors affecting carbon emissions of land holdings include the share of primary industry output, land area per capita, and land use index (Narit et al. 2016).

However, nighttime light remote sensing data is inconsistent in different years, and the detection performance will gradually weaken, leading to problem like discontinuous image data (Liu et al. 2022). It has also been shown that nighttime lighting data are better suited to describe population activity, but not for reflecting energy consumption and CO₂ emissions (Zhang et al. 2021). Furthermore, there were some studies generated fossil fuel carbon emissions at grid scale. Yang et al. (2022) simulated the spatial distribution of CO₂ emissions based on fossil fuel carbon emission grid data and land use data. Gurney et al. (2020) used the carbon

emission survey results of industry, commerce, household consumption, and other industries in American to form a carbon emission product at 1-km resolution. However, this method cannot be applied widely to detect the spatial distribution of carbon emissions due to difficulties in energy data availability and validity (Huynh et al. 2017).

Spatial heterogeneity refers to the unevenness and complexity of the spatial distribution of ecological processes and patterns, which can be generally understood as the sum of patchiness and gradient (Zhenyue et al. 2023). To distinguish the spatial heterogeneity of CO₂ emissions, many studies take land use type as the basic unit for carbon emission calculation (Xiaowei and Jianxi 2019; Zeng et al. 2022). For instance, Muntean et al. (2014) used land use and human activity data to build a global greenhouse gas emission dataset with 0.1° resolution from 1970 to 2008 and tried to reduce CO₂ emissions by optimizing the structure of land use (Li et al. 2022). However, in the existing studies on land use CO₂ emissions, most of them only took into account the differences between built and non-built land and ignored the carbon intensity in detail between different functional areas, such as transport land, commercial land, and industrial land (Wang et al. 2019; Upadhyay et al. 2021). As the carbon emission intensity is significantly diverse with these different functional areas, it is necessary to further explore the difference of CO₂ emissions among different functional areas.

UFZs describe the human activities within a certain area and contain socio-economic characteristics (Zhu et al. 2022). As the most basic unit of urban development, UFZ reflects the socio-economic characteristics of a specific region and helps to realize the optimization of energy consumption. Through it, the allocation of public resources and the type of energy consumption can be clearly observed. All functional areas are aggregated by geographic objects and extracted from the land use, and the same functional zone has basically similar energy consumption and carbon metabolism patterns (Wang et al. 2022a). Relatively speaking, the estimation of CO₂ emissions at the UFZ scale can help urban planners to anticipate the carbon emissions associated with urban development. Thus, UFZs are a reasonable basic unit for the estimation of CO₂ emissions (Jing et al. 2022; Zheng et al. 2022). The explosive growth of urban big data like social media data, cell phone signaling data, and point-of-interest (POI) data is characterized by large sample size and rich types, which makes up for the poor recognition ability of remote sensing technology on urban functional interaction and can help accurately detect the spatial distribution of UFZs (Zhou 2022), so as to promote the refined research on urban carbon emissions.

This study further constructed a framework to estimate the spatial pattern of CO₂ emissions based on the scale of UFZs, using the land use type as the basic unit, in the case of Pudong New Area, Shanghai, China. Firstly, we extracted

UFZs by combining remote sensing image with POI and road network data. Then, the carbon emissions of each UFZ were obtained through the combination of top-down decomposition and bottom-up spatial estimation method. Finally, the spatial patterns of CO₂ emissions at the UFZ scale were analyzed to provide policy implications for the process of building a low carbon city. Overall, this study mapped the spatial distribution of CO₂ emissions intensity at the UFZ scale, which is necessary for urban planning to adjust and reshape the industrial layout to build a more sustainable city.

Data and methods

Study area

Pudong New Area is located in the eastern part of Shanghai, with an area of 1210 km², making it the largest municipal district in Shanghai (Fig. 1). Since the reform and opening up, Pudong New Area has experienced rapid urban development, a huge economic volume and extremely frequent human activities (Gong et al. 2022b). It is also an important transportation hub with a three-dimensional integrated transportation system including international ports, railway transport, air transport, and intercity high-speed transport, etc. (Qingyu and Oh 2021). The huge energy consumption has increased the corresponding carbon emissions year by year. As one of the most well-developed zones in China, Pudong New Area has played an indispensable role in the transition to an energy efficient and low emission mode. Therefore, this study chose Pudong New Area as a typical case area.

Data source and preprocessing

Data source

POI is the most important element of population agglomeration, which can better reflect the spatial distribution of material resources in the city, but its spatial distribution pattern is different (Yang and Li, 2022). POI opens up a new way of thinking for the study of urban spatial structure, and it has been widely used in the fields of analysis of the spatial pattern of UFZs (Xia et al. 2022). Multiple-source data were used to estimate UFZ scale based on energy consumption and CO₂ emissions in Pudong. Specifically, the POI data was obtained from the Gaode Map Open Platform in 2019. And the road network data was obtained from the map sharing plan OpenStreetMap (OSM) website. Energy consumption and other data related to CO₂ emission calculation were provided by China Energy Statistical Yearbook and Pudong New Area Statistics Bureau.

Data preprocessing

There were about 201 thousand POI data of all categories in Pudong New Area, and major types of use cover sightseeing spots, enterprises, traffic devices, education, medical care, community activities, business residence, etc. During the collection process, there were some problems, such as duplication of raw data and missing data, which cannot be used directly. Thus, therefore, missing data should be added, and duplicate data should be deleted and reclassified. In addition, since the actual OSM data obtained had topological errors,

Fig. 1 Overview map of the study area

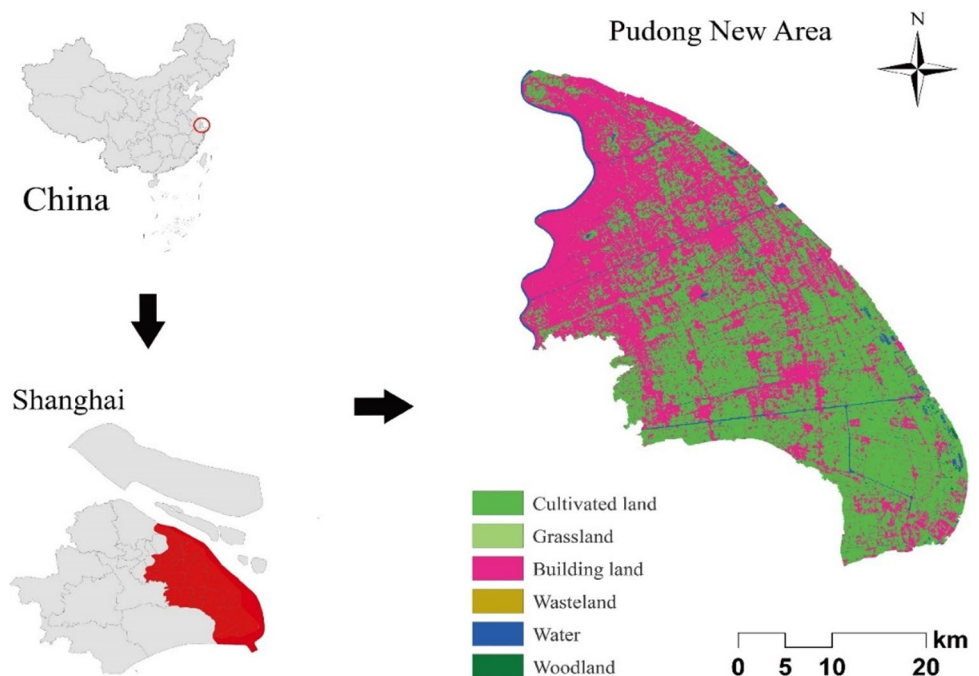
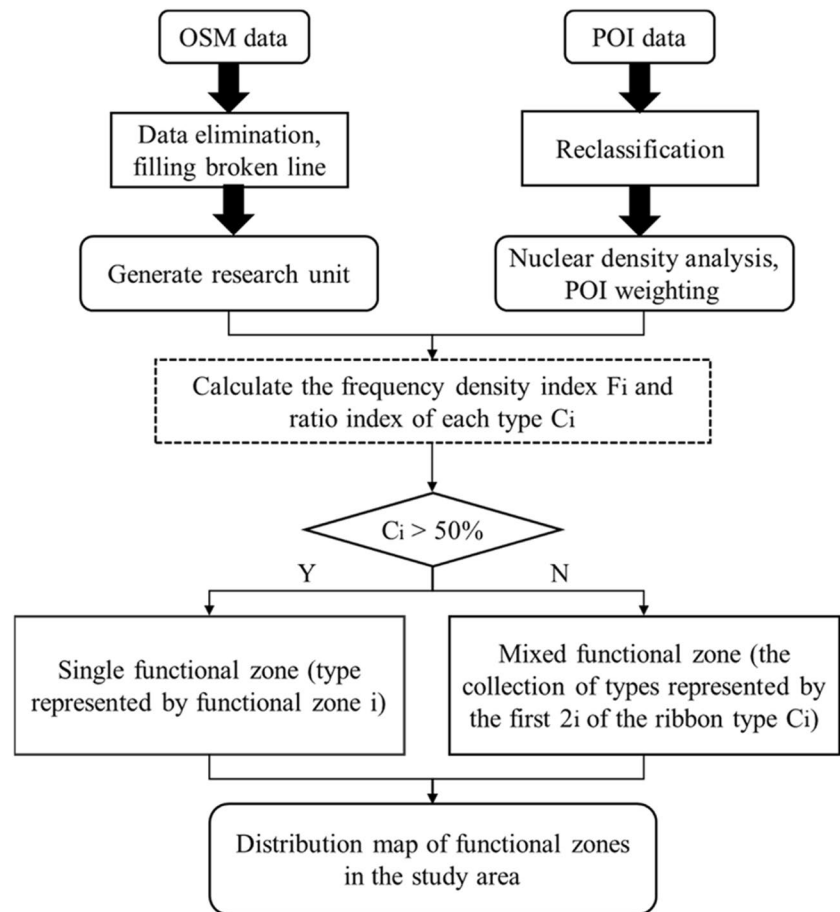


Fig. 2 The flow chart of UFZs identification



there were a large number of dead ends, redundant cross roads, and unsealed roads that were not usable. Therefore, it is necessary to preprocess the road data in combination with the high-resolution images and select the main highways, trunk roads, urban primary roads, secondary roads, etc.

Methods

UFZ extraction and verification

Extraction of single UFZs Figure 2 demonstrates the process of UFZs identification. All the POI data were divided into six types according to the land use type: industrial (ID) zone, transport (TS) zone, residential (RS) zone, cultural tourism (CT) zone, commercial service (CS) zone, and public service (PS) zone. The frequency density and proportion of different POI types can be directly used to reflect the type of urban function. The frequency density can be expressed as

$$F_i = \frac{n_i}{S_i} (i = 1, 2, \dots, 6) \quad (1)$$

where i represents the type of POI and n_i represents the quantity of the different POI types, S_i represents the total

number of the different POI types, and F_i represents the frequency density of the different POI types in the total number of POIs.

In order to compare different types of POI, C_i vector was used to represent the proportion of each type of POI in the unit on the basis of density. The calculation formula is as follows:

$$C_i = \frac{F_i}{\sum_{i=1}^6 F_i} \times 100\% (i = 1, 2, \dots, 6) \quad (2)$$

According to the calculation results of C_i , the POI and the research unit were superposed and analyzed to build the underlying data of urban spatial pattern, the hooking point data, and the street unit. And the POI-related data was calculated through the field calculator.

Extraction of mixed UFZs In the actual practice, many UFZs usually hold mixed functions. Concretely, this study defined the unit as a single functional area when the proportion of the POI type was greater than or equal to 50%. On the contrary, when the proportion of the POI type was less than 50%, it was determined that there was not dominant UFZ in this area, which meant it was mixed

UFZ. When the proportion of all the POI types was less than 20%, it was considered an integrated UFZ. Since the integrated UFZ occupied little proportion of the study area, it was not considered in this study.

Accuracy evaluation of UFZ extraction results For accuracy evaluation, this study selected some units and verified the UFZ classification by sampling and scoring. Specifically, the full score was set up to 3, meaning complete consistency, while 0 meant complete inconsistency. If a single UFZ was identified as a mixed UFZ, the score was 2. And if a mixed UFZ was identified as a single UFZ included in the corresponding mixed UFZ, or as a mixed UFZ containing a function included in the corresponding mixed UFZ, the score was 2. The calculation formula for precision evaluation is as follows:

$$A = \frac{\sum_{i=1}^n x_i}{\sum_{i=1}^n X_i} \times 100\% \tag{3}$$

where A is the verification accuracy of UFZ, x_i is the score of randomly selected sample, and X_i is the total score of randomly selected samples.

Calculation of CO₂ emissions at the UFZ scale

Calculation of CO₂ emissions in industrial zones Based on

Table 1 Conversion between passenger and cargo and CO₂ emission coefficient

Mode of transportation	Passenger transport conversion factor	CO ₂ emission coefficient
Highway	1 P km = 1 T km	0.1955
Railway	13 P km = 1 T km	9.6000
Water transport	10 P km = 1 T km	0.5560
Aviation	3 P km = 1 T km	0.0425

the range of CO₂ emissions from energy consumption, this study adopted the top-down accounting method to calculate CO₂ emissions in industrial zones. The construction model is as follows:

$$CP = \sum_i C_i \times \sum_i EF_i \tag{4}$$

where CP is the total CO₂ emissions generated by the functional area, i is the energy type, C is the amount of energy consumption, and EF_i is the CO₂ emission coefficient of energy i .

Calculation of CO₂ emissions in residential and commercial service zones As the carbon emission sources in residential zones and commercial service zones are mainly liquefied petroleum gas, electricity, gas, coal, etc. and the energy consumption data is difficult to obtain, this study utilized carbon emission intensity obtained from previous research to calculate the CO₂ emissions in residential zones and commercial service zones. Its calculation formula is as follows:

$$CO_{2m} = \sum_{i=1}^n (k_i \times E_i \times d_i) \tag{5}$$

where CO_{2m} is the total amount of various CO₂ emissions of these zones, i is the energy consumption category, k_i is the conversion factor for different energies, E_i is the amount of energy consumption of category i , and d_i is the CO₂ emission coefficient (constant value).

Calculation of CO₂ emissions in public service and cultural tourism zones

The carbon emission accounting of public service zones and cultural tourism zones referred to the previous studies, which used the carbon emission intensity to estimate the CO₂ emissions in the corresponding zones (Gao and Li 2021). The general calculation model is as follows:

$$C = \sum (L_j A_j) \tag{6}$$

where C is the CO₂ emissions of UFZ, j is the UFZ type, A_j is the area of UFZ, and L_j is the CO₂ intensity of UFZ.

Calculation of CO₂ emissions in transport zones

This study adopted the carbon emission coefficient of four transportation modes, namely, railway, highway, water transport, and aviation (Table 1) to calculate the carbon emissions:

$$CO_{2T} = CO_{2T1} + CO_{2T2} \tag{7}$$

$$CO_{2T1} = \sum (g_{1i} \times h_i + g_{2i}) \times k_i \tag{8}$$

$$CO_{2T2} = \alpha CO_{2T1} \tag{9}$$

where CO_{2T} is the total CO₂ emissions of the transportation system, CO_{2T1} is the total CO₂ emissions from intercity transportation, and CO_{2T2} is the total CO₂ emissions of urban passenger transportation, i is different types of transportation modes, g_{1i} is the passenger turnover, g_{2i} is the freight turnover, k_i is the passenger cargo conversion coefficient, and α is the carbon emission ratio coefficient of intercity transportation and urban transportation.

Spatial pattern analysis of UFZ based on carbon emissions

Utilizing the reclassified POI and OSM data and combining the carbon emission accounting data of each UFZ, the carbon emission maps of residential zones, commercial service zones, industrial zones, and transport zones were conducted as follows:

$$CO_{2i} = \frac{D_i \times C}{\sum_{i=1}^n D_i} \quad (10)$$

where CO_{2i} is the CO_2 emission value of UFZ, D_i is the carbon emission intensity of UFZ, n is the total number of pixels in the study area, and C is the total CO_2 emission of all the UFZs.

According to the spatial distribution of POI in each UFZ and the relevant energy consumption, the CO_2 emission intensity of residential zones, industrial zones, and commercial service zones was calculated as follows:

$$P = \frac{\sum_{i=1}^n W_i}{A} \quad (11)$$

where P is the carbon emission intensity, W_i is the emission weight of POI in corresponding UFZs (the weight of residential zones, commercial service zones, industrial zones, and tertiary industry is 1, respectively), A is the total area of UFZ, and n is the total amount of POI in certain UFZ.

As the transport zone is a linear vector, its calculation model of CO_2 emission intensity is as follows:

$$D = \frac{\sum_{i=1}^m L_i \times W_i}{A} \quad (12)$$

where D is the CO_2 emission intensity, L_i is the length of the road in the UFZ within the search range, W_i is the volume of traffic on the road, A is the total area, and m is the total number of roads in the search range.

Exploratory spatial data analysis (ESDA) describes and visualizes the spatial characteristics of data by establishing statistical relationships through spatial geographic location correlation, so as to recognize the characteristics of data spatial distribution and to explore spatial correlation information. Spatial autocorrelation analysis is the main module of ESDA, which reveals the degree of interdependence between data from different geographical locations. According to the mutual spatial relationship, it can be divided into positive correlation and negative correlation. According to the scope of study, it can be classified into two categories: global spatial autocorrelation and local spatial autocorrelation.

Global spatial autocorrelation analysis

Global Moran's I is a key index used to assess the global applicability of spatial data, and it takes values between -1 and 1 . When $I < 0$, it means that there is a negative spatial correlation in the distribution of this spatial element, and its negative correlation is stronger when the value of I is closer to -1 . When $I > 0$, it means that there is a positive spatial correlation, and its positive correlation is stronger when the value of I is closer to 1 . When $I = 0$, it means that these are spatially randomly distributed and do not have any spatial correlation. In the study, Global Moran's I calculation formula for urban carbon emissions is as follows:

$$I = \frac{n \sum_{i=1}^n \sum_{j=1}^n w_{ij} (x_i - \bar{x})(x_j - \bar{x})}{\left(\sum_{i=1}^n \sum_{j=1}^n w_{ij} \right) \sum_{i=1}^n (x_i - \bar{x})^2} \quad (13)$$

where I denotes Global Moran's I , n denotes the total number of regions, x_i is the CO_2 emissions of region i , x_j is the CO_2 emissions of region j , \bar{x} is the average CO_2 emissions, and w_{ij} is the normalized spatial weight matrix (Eq. (14)), which characterizes the neighborhood relationship between spatial objects. There are two types of spatial weight matrix, Rook and Queen. Rook denotes the adjacency of common edges, and Queen denotes the adjacency of common vertices. In the study, Queen adjacency was used, that is, if region i and region j have a common edge, $w_{ij} = 1$; otherwise, $w_{ij} = 0$.

$$w_{ij} = \begin{bmatrix} w_{11} & \cdots & w_{j1} \\ \vdots & \ddots & \vdots \\ w_{i1} & \cdots & w_{jn} \end{bmatrix} \quad (14)$$

By standardizing the Z value and P value, the significance of Global Moran's I can be evaluated. The null hypothesis of no spatial autocorrelation among spatial elements is first established, and the decision to reject or accept the null hypothesis is made by comparing the P value with the significance level: if $-1.96 < Z < 1.96$ and $P > 0.05$, the null hypothesis is accepted; if $Z \geq 1.96$ or $Z \leq -1.96$ with $P \leq 0.05$, the null hypothesis is rejected. The Z value was calculated as

$$Z(I) = \frac{I - E(I)}{\sqrt{\text{VAR}(I)}} \quad (15)$$

and

$$E(I) = \frac{1}{n-1} \quad (16)$$

where $E(I)$ is the theoretical expected value and $\sqrt{\text{VAR}(I)}$ is the theoretical variance.

Moran’s scatter plot is a visualization result of global autocorrelation analysis, which can visualize the type of spatial autocorrelation each spatial element, respectively, and qualitatively reveal the local spatial stability of the study object. It represents different types of spatial agglomerations in four quadrants in the form of Cartesian coordinate system: high-high (H-H), low-low (L-L), high-low (H-L), and low-high (L-H).

Local spatial autocorrelation analysis

Global Moran’s *I* can identify the overall spatiality of the study object, and Moran’s scatter plot can indicate the type of agglomeration of each spatial element, but neither of them can show the specific spatial location of the agglomeration. In the study, the Local Indicators of Spatial Association (LISA) index was further used to analyze the local spatial pattern of the urban CO₂ emissions. The principle of LISA index is to decompose Global Moran’s *I* into various parts of the entire spatial range, which can effectively reveal the aggregation of various spatial elements at specific locations. The formula is as follows:

$$I_i = \frac{x_i - \bar{x}}{S} \sum_{j=1}^n W_{ij}(x_j - \bar{x}) \tag{17}$$

where

$$S = \left(\sum_{j=1, j \neq i}^n x_j^2 / (n - 1) \right) \bar{x}^2 \tag{18}$$

while the rest of the variables have the same meaning as in Eq. (13).

Results and discussion

Results and validation of UFZ extraction

Figure 3 shows the distribution of processed POI data excavated from Gaode Map. Among them, commercial service, residential, and public service POIs were most densely distributed in the center of Pudong New Area, while industrial POIs were concentrated in their surroundings. And the transport POIs were mostly concentrated in coastal ports, airports, and high-speed railway stations, with the cultural tourism POIs distributed far away from the urban center.

Figure 4 shows the proportion of single UFZs and mixed UFZs, respectively. Thus, for single UFZs, transport and industrial zones accounted for 63%; for mixed UFZs, those with transport or industrial zones accounted for the majority at 76%. The results of UFZ extraction showed that there were 1083 functional zones, of which 124 single UFZs accounted for 11.45% and 959 mixed UFZs accounted for 88.55% (Fig. 5). Concretely, mixed UFZs were mainly distributed in areas with developed economy, complete infrastructure, and convenient life.

Generally, residential zones were mainly located in larger towns away from commercial centers. Similarly, in this study, most of the residential areas in Pudong were located in the old urban areas around the center, with small plots and many patches. Commercial service zones were

Fig. 3 Distribution of various POIs in the study area

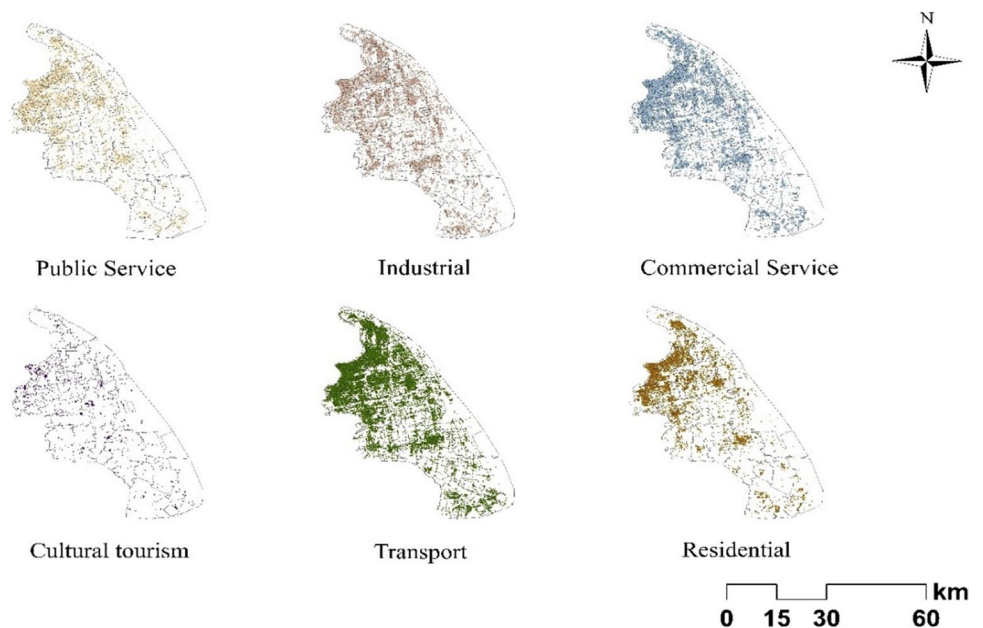


Fig. 4 The proportion of different UFZs (a represents the proportion of single UFZ and b represents the proportion of mixed UFZ)

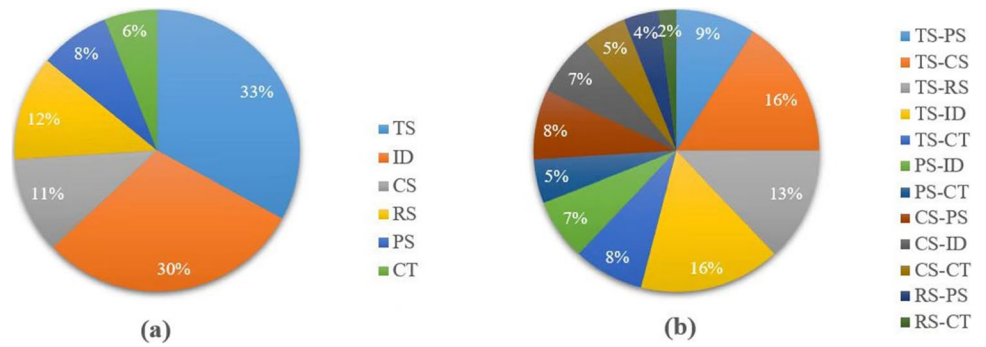
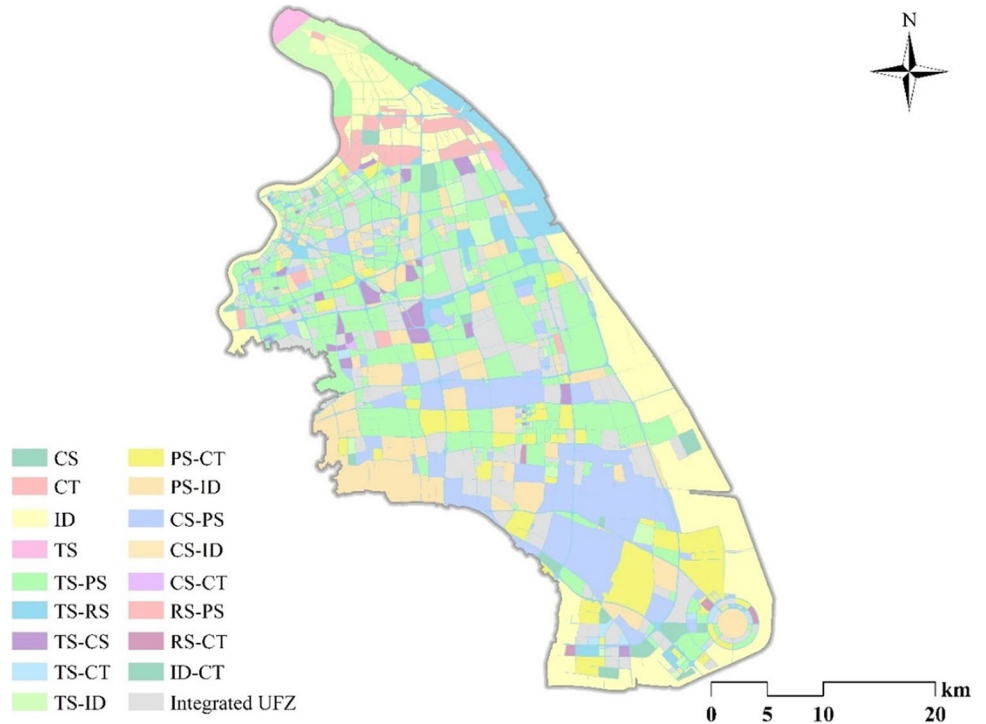


Fig. 5 UFZ identification results of the study area



located around large business districts, that is, in the center of Pudong or around the Huangpu River, providing support for citizens' life services. Industrial zones were located in the southeast and southwest of Pudong, with obvious industrial function advantages and intensive production factors. Public service zones were mainly located around administrative organs, like education, culture, and medical facilities. Transport zones were mainly located in Pudong Airport, railway station, subway, port, and other large transport hub areas (Zhao et al. 2022).

Compared with the existing research conducted in the other cities (Chen et al. 2022), the single UFZs of this study area accounted for 63% of the total. That is mainly because the UFZs in Pudong were concentrated in the central area, or around coastal ports and other peripheral areas, different UFZs had a high degree of overlap. In addition, in terms of research methods, we divided UFZs by constructing

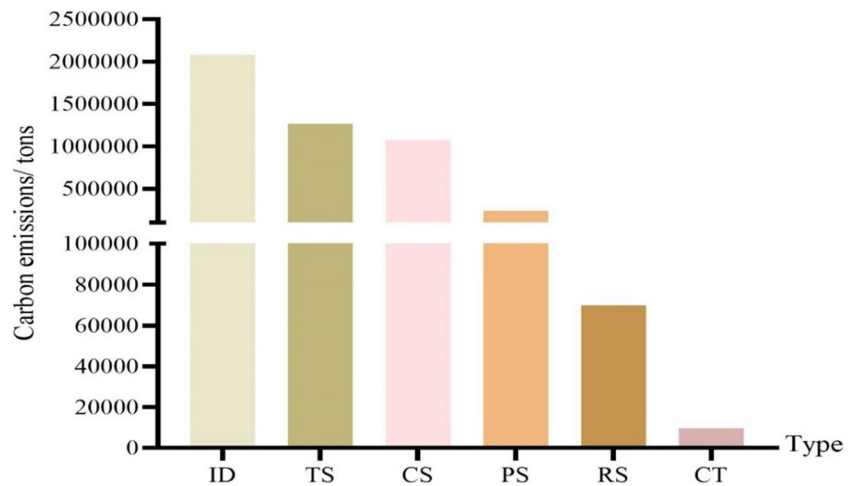
Table 2 Verification score of functional zone identification

Score	3	2	1	0
Number of points	192	57	40	11
Total score	576	114	40	0

frequency density vectors based on POI and OSM data, while the above research divided UFZs through pixel threshold method based on POI and land use data. This was different from our situation, because Pudong was relatively developed in economy, commerce, and transportation; it was difficult to use the threshold method to divide various functional categories in the road network.

For precision evaluation, 300 UFZs were randomly selected and compared with the real map. The score was shown in Table 2. The overall accuracy was 81.1%, meeting

Fig. 6 CO₂ emissions of the six UFZs



the experimental requirements. This indicated that the POI data can supplement the remote sensing data and improve the spatial refinement.

Results of urban CO₂ emission accounting

Figure 6 shows the carbon emissions of each UFZ, with the industrial, transport, and commercial service zones ranking in the top 3, while the residential and cultural tourism zones were far below them. This is consistent with the existing studies (Wang et al. 2022b), which computed the CO₂ emissions of various functional zones in Sichuan province and found out that the percentage of CO₂ emissions in industrial zones and transport zones was much higher than those in other UFZs.

According to the framework of IPCC, the carbon emission sources of industrial zones include emissions in the production process, waste treatment, and changes in land use (Mir et al. 2021; Xu et al. 2021). Therefore, due to the limited availability of data, the CO₂ emissions of some UFZs may be underestimated, and the total carbon emissions considered in this study may be slightly lower than the actual values. Nevertheless, compared with the bottom-up carbon emission accounting, the top-down method used in this study covered all the energy consumption, which may in turn improve the estimate accuracy (Chen et al. 2023). Overall, the CO₂ emissions computed in this study were obtained from statistical data due to the additional time required for field surveys, but the emissions results were relatively feasible and valid.

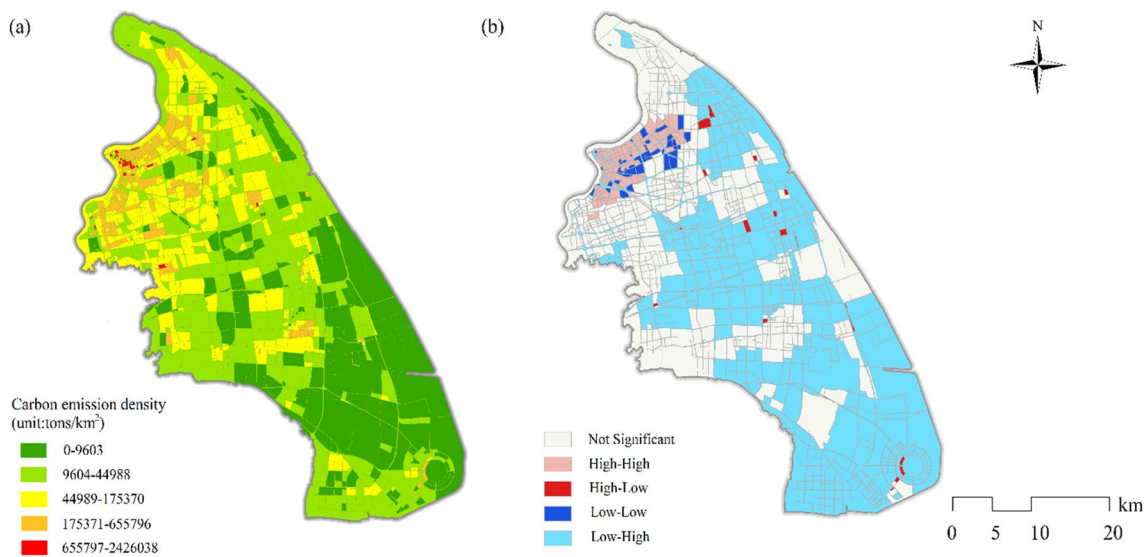


Fig. 7 The spatial distribution of CO₂ emissions (a) and the local spatial autocorrelation analysis (b)

Spatial patterns of UFZs based on CO₂ emissions

Spatial distribution

The spatial distribution of CO₂ emissions at the UFZ scale was shown in Fig. 7. In terms of spatial distribution, the CO₂ emissions of industrial zones ranked first, because China's economy still mainly relied heavily on industry. Therefore, the adjustment of the structure of industrial UFZs was crucial for carbon emission reduction. Secondly, the emission source generated by the industrial zones was also the main source of air pollutants, which greatly affected the human living environment (Ahmed et al. 2022; Piotr and Zbigniew 2015). Therefore, in urban planning, the relevant environmental agencies must strictly monitor the CO₂ emissions generated by the design of the spatial distribution of industrial land.

The transport zones were the second largest source area of urban CO₂ emissions (Zhou et al. 2023), as the regional traffic facilities have undertaken the transportation task of serving the normal economic development of Pudong, especially the existence of numerous ports, which makes Pudong a world shipping node. Therefore, it should be properly adjusted the distribution of transport zones in the urban space, such as increasing the strength of water transportation to replace part of air transportation, in order to achieve the goal of reducing CO₂ emissions from transportation (Wang et al. 2023).

Spatial autocorrelation

The global spatial autocorrelation analysis showed that Moran's *I* value was 0.8116, which revealed that the positive correlation of urban carbon emissions in Pudong New Area was stronger in terms of spatial distribution. And the CO₂ emissions of high and low carbon intensity regions were more significantly different from other regions. Furtherly, local spatial autocorrelation results illustrated that industrial zones and transport zones were the main locations of high emission concentrations in Fig. 7. In the LISA cluster map, high-high, high-low, and low-high clusters were majorly distributed in inland ports and areas around the city center. This was because inland ports were important transportation hubs in Pudong, while industrial enterprises were distributed in areas around the city center, which was the same as the location of these clusters in the LISA map. Besides, low-low clusters were majorly distributed in coastal areas and areas far from urban centers (Xia et al. 2023). This was mainly due to the fact that these areas have poorer economies and fewer large shopping malls (Zhu et al. 2023). And because of the large

area, there was more agricultural and forestry land and parkland.

Compared with the extraction results of UFZs, it can be found that the areas with high carbon emissions were mainly located in the center of Pudong New Area and inland ports, while the areas with low carbon emission intensity were mainly located in coastal communities, such as Chuansha New Town and other areas with good ecological environment quality. Existing research failed to accurately show the difference in regional carbon emissions (Ji and Lin 2022; Zhou et al. 2023); this study took the impact of UFZ into account, so as to simulate regional carbon emissions distribution at a finer scale.

Conclusion

It is crucial to make accurate spatial distribution simulations of urban CO₂ emissions for low carbon city construction. The study used POI and road network data to extract UFZs in Pudong New Area, China, and designed a framework based on the scale of UFZs to explore the spatial distribution pattern of CO₂ emissions. The results showed that the spatial difference of the mixed utilization degree of the UFZs was obvious within the study area, which was specifically reflected in the downtown area, especially in the areas with developed transportation. Accordingly, there were significant spatial differences in urban CO₂ emissions at the UFZ scale (Li et al. 2021; Xia et al. 2022). Specifically, the high CO₂ emission areas were located in the typical secondary industry and transport functional areas around the inland ports and urban center, which was consistent with the actual situation (Tao et al. 2023; Yang et al. 2023). Besides, in terms of spatial autocorrelation analysis, the CO₂ emissions in Pudong New Area presented a significant high spatial agglomeration, and the high CO₂ emission clusters were majorly distributed in the zones with concentrated industries and transportation. This paper tried to decompose the CO₂ emissions into corresponding UFZs and established the UFZ carbon emission correlation framework, fully considering the spatial heterogeneity within the area, which can help improve the policy implementation for low carbon city construction (Wang et al. 2018).

At present, the POI data used in this study only included the location, name, type, etc., while the corresponding housing area of each UFZ needed to be supplemented in the subsequent research. Furthermore, high-resolution remote sensing images can be utilized to obtain building profiles. And with the maturity of big data and artificial intelligence technology, future research can try to extend UFZ-based carbon emission spatialization to larger scope.

Acknowledgements This research was supported by the National Natural Science Foundation of China (No.72104139)

Author contribution EZ wrote the manuscript and offered funding to support the research. JY wrote the manuscript and created the tables and figures. XZ collected and analyzed the data. LC provided experimental guidance. All the authors have read and approved the final manuscript.

Funding This research was supported by the National Natural Science Foundation of China (No. 72104139) and (No.71972128).

Data availability The datasets used during the current study are available from the corresponding author on reasonable request.

Declarations

Ethics approval Not applicable.

Consent to participate Not applicable.

Consent for publication Not applicable.

Competing interests The authors declare no competing interests.

References

- AbdelRahman MAE et al (2021) Assessment of land degradation using comprehensive geostatistical approach and remote sensing data in GIS-model builder. *Egypt J Remote Sens Space Sci* 22(3):323–334
- Ahmed J et al (2022) Urban air pollution caused of particulate matter and lead in the City of Chittagong-Bangladesh. *Am J Environ Sci Eng* 6(1):7–15
- Chen L, Qi Q, Wu H et al (2023) Will the landscape composition and socio-economic development of coastal cities have an impact on the marine cooling effect? *Sustain Cities Soc* 89:104328
- Chen Y et al (2022) A GloVe model for urban functional area identification considering nonlinear spatial relationships between points of interest. *ISPRS Int J Geo-Inf* 11(10):498
- Gan L et al (2022) Regional inequality in the carbon emission intensity of public buildings in China. *Buil Environ* 225:109657
- Gao N, Li F (2021) Spatial quantitative analysis of urban energy consumption based on POI and night-time remote sensing data. *Int J Econ Energy Environ* 6(6):164–173
- Gong W et al (2023) Analysis of urban carbon emission efficiency and influencing factors in the Yellow River Basin. *Environ Sci Pollut Res Int* 30(6):14641–14655
- Gong Y, et al (2022) Assessing changes in the ecosystem services value in response to land-use/land-cover dynamics in Shanghai from 2000 to 2020. *Int J Environ Res Public Health* 19(19)
- Gurney, K et al (2020) The vulcan version 3.0 high-resolution fossil fuel CO₂ emissions for the United States. *J Geophys Res-Atmos* 125(19):e2020JD032974
- Hu G, Ma X, Ji J (2019) Scenarios and policies for sustainable urban energy development based on LEAP model – A case study of a postindustrial city: Shenzhen China. *Appl Energy* 238:876–886
- Huynh LH et al (2017) Developing a high-resolution melting method for genotyping and predicting association of SNP rs353291 with breast cancer in the Vietnamese population. *Biomed Res Therapy* 4(12):1812–1831
- Ji J, Lin H (2022) Evaluating regional carbon inequality and its dependence with carbon efficiency: implications for carbon neutrality. *Energies* 15(19)
- Jing Y, Sun R, Chen L (2022) A method for identifying urban functional zones based on landscape types and human activities. *Sustainability* 14(7):1430
- Li W et al (2022) Spatiotemporal evolution of county-level land use structure in the context of urban shrinkage: evidence from Northeast China. *Land* 11(10):1709
- Li Y, Shen J, Xia C et al (2021) The impact of urban scale on carbon metabolism—a case study of Hangzhou, China[J]. *J. Clean Prod* 292:126055
- Liu H et al (2022) Identification of relative poverty based on 2012–2020 NPP/VIIRS night light data: in the area surrounding Beijing and Tianjin in China. *Sustainability* 14(9):5599
- Muntean M et al (2014) Trend analysis from 1970 to 2008 and model evaluation of EDGARv4 global gridded anthropogenic mercury emissions. *Sci Total Environ* 494–495:337–350
- Mir KA et al (2021) Comparative analysis of greenhouse gas emission inventory for Pakistan: part II agriculture, forestry and other land use and waste. *Adv Clim Chang Res* 12(1):132–144
- Narit Y, Sithichai L, Benjavan R (2016) Carbon storage in mountain land use systems in Northern Thailand. *Mt Res Dev* 36(2):183–192
- Oda T, Maksyutov S (2011) A very high-resolution (1 km×1 km) global fossil fuel CO₂ emission inventory derived using a point source database and satellite observations of nighttime lights. *Atmos Chem Phys* 11(219):543–556
- Piotr H, Zbigniew N (2015) Emission data uncertainty in urban air quality modeling—case study. *Environ Model Assess* 20(6):583–597
- Qingyu Q, Oh KK (2021) Exploring the characteristics of high-speed rail and air transportation networks in China: a weighted network approach. *J Int Logist Trade* 19(2):96–114
- Tao W, Kai Z, Keliang L et al (2023) Spatial heterogeneity and scale effects of transportation carbon emission-influencing factors—an empirical analysis based on 286 cities in China. *Int J Environ Res Public Health* 20(3):2307
- Upadhyay S et al (2021) Spatio-temporal variability in soil CO₂ efflux and regulatory physicochemical parameters from the tropical urban natural and anthropogenic land use classes. *J Environ Manag* 295:113141
- Wang P et al (2017) Analysis of energy consumption in Hunan Province (China) using a LMDI method based LEAP model. *Energy Procedia* 142:3160–3169
- Wang L et al (2022a) Stackelberg game-based optimal scheduling of integrated energy systems considering differences in heat demand across multi-functional areas. *Energy Rep* 8:11885–11898
- Wang G, Han Q, de Vries B (2019) Assessment of the relation between land use and carbon emission in Eindhoven, the Netherlands. *J Environ Manag* 247:413–424
- Wang SH, Huang SL, Huang PJ (2018) Can spatial planning really mitigate carbon dioxide emissions in urban areas? A case study in Taipei, Taiwan. *Landsc Urban Plan* 169:22–36
- Wang T et al (2023) Spatial heterogeneity and scale effects of transportation carbon emission-influencing factors—an empirical analysis based on 286 cities in China. *Int J Environ Res Public Health* 20(3):2307
- Wang X et al (2022b) Carbon emission accounting and spatial distribution of industrial entities in Beijing—Combining nighttime light data and urban functional areas. *Eco Inform.* 70:101759
- Wang Z et al (2017) Monitoring evolving urban cluster systems using DMSP/OLS nighttime light data: a case study of the Yangtze River Delta region, China. *J Appl Remote Sens* 11(04)
- Xia C, Dong Z, Wu P et al (2022) How urban land-use intensity affected CO₂ emissions at the county level: Influence and prediction[J]. *Ecol Indic* 145:109601

- Xia C, Zhang J et al (2023) Exploring potential of urban land-use management on carbon emissions—A case of Hangzhou, China[J]. *Ecol Indic*. 146:109902
- Xia S, Yang Y (2022) Examining spatio-temporal variations in carbon budget and carbon compensation zoning in Beijing-Tianjin-Hebei urban agglomeration based on major functional zones. *J Geogr Sci* 32(10):1911–1934
- Xiaowei C, Jianxi F (2019) High resolution carbon emissions simulation and spatial heterogeneity analysis based on big data in Nanjing City, China. *Sci Total Environ* 686:828–837
- Xu R et al (2021) Magnitude and uncertainty of nitrous oxide emissions from North America based on bottom-up and top-down approaches: informing future research and national inventories. *Geophys Res Lett* 48(23):e2021GL095264
- Yang R, Hu Z, Hu S (2023) The failure of collaborative agglomeration: from the perspective of industrial pollution emission. *J Clean Prod* 387:135952
- Yang T et al (2022) An estimating method for carbon emissions of China based on nighttime lights remote sensing satellite images. *Sustainability* 14(4):2269
- Yang Y, Li H (2022) Monitoring spatiotemporal characteristics of land-use carbon emissions and their driving mechanisms in the Yellow River Delta: a grid-scale analysis. *Environ Res* 214(P4):114151
- Zeng L et al (2022) The carbon emission intensity of industrial land in China: spatiotemporal characteristics and driving factors. *Land* 11(8):1156
- Zhang Q et al (2022) Using multi-source geospatial information to reduce the saturation problem of DMSP/OLS nighttime light data. *Remote Sens* 14(14):3264
- Zhang Y et al (2021) Spatial-temporal characteristics and decoupling effects of China's carbon footprint based on multi-source data. *J Geogr Sci* 31(3):32614–32627
- Zheng Y et al (2022) Estimating carbon emissions in urban functional zones using multi-source data: a case study in Beijing. *Build Environ* 212:108804
- Zhenyue L, Jinbing Z, Pengyan Z et al (2023) Spatial heterogeneity and scenario simulation of carbon budget on provincial scale in China. *Carbon Balance Manag* 18(1):20
- Zhou K et al (2023) Spatial and temporal evolution characteristics and spillover effects of China's regional carbon emissions. *J Environ Manag* 325(PA):116423
- Zhou N (2022) Research on urban spatial structure based on the dual constraints of geographic environment and POI big data. *J King Saud University-Sci* 34(3):101887
- Zhao J, Shao Z, Xia C et al (2022) Ecosystem services assessment based on land use simulation: A case study in the Heihe River Basin, China[J]. *Ecol Indic* 143:109402
- Zhu E et al (2022) The spatial-temporal patterns and multiple driving mechanisms of carbon emissions in the process of urbanization: a case study in Zhejiang, China. *J Clean Prod* 358:131954
- Zhu E et al (2023) Spatiotemporal coupling analysis of land urbanization and carbon emissions: A case study of Zhejiang Province, China. *Land Degrad Dev* 34:4594–4606

Publisher's Note Springer Nature remains neutral with regard to jurisdictional claims in published maps and institutional affiliations.

Springer Nature or its licensor (e.g. a society or other partner) holds exclusive rights to this article under a publishing agreement with the author(s) or other rightsholder(s); author self-archiving of the accepted manuscript version of this article is solely governed by the terms of such publishing agreement and applicable law.